

Chemical Abundances and Yields from Massive Stars

André Maeder, Georges Meynet & Raphael Hirschi

Geneva Observatory, CH-1290 Sauverny, Switzerland

Abstract. Stellar rotation produces an internal mixing of the elements due to shear instability and meridional circulation. This leads to observable N/C enhancements in massive stars above about $7\text{--}9 M_{\odot}$. Rotation also favours mass loss by stellar winds. Mass loss effects dominate for masses above $30 M_{\odot}$, while mixing dominates below that limit. The effects of mixing are also much larger at lower metallicity Z , because the internal Ω -gradients are steeper. This appears to be in agreement with observations in the SMC.

At very low Z and $Z = 0$, mixing between the He-burning core and the H-burning shell leads to the production of primary N in intermediate mass stars. Such enrichments increase the metallicity of the rotating star, also massive $Z = 0$ stars with moderate initial velocities currently reach break-up velocity during a fraction of the MS phase. Both effects favour mass loss in $Z = 0$ stars, which have ejecta with abundance anomalies very similar to those of C-rich very metal poor stars.

1. Introduction

David Lambert has made major contributions to our knowledge of chemical abundances in all kinds of stars. Chemical abundances are the most decisive test on mixing in stellar evolution, which affects all model outputs: tracks, lifetimes, stellar winds, supernovae progenitors, star populations in galaxies, nucleosynthesis and yields, etc. Thus, the abundance determinations made by David Lambert are an essential piece of our astrophysical knowledge.

Here, we examine the case of massive stars, where rotation and mass loss play a major role. Noticeably, several results of models at low metallicity Z also have implication for the abundances of very metal poor halo stars.

2. Basic physical ingredients concerning rotation and mass loss

We briefly summarize the physical assumptions about the treatment of mass loss and rotation in stellar models.

Structure: We consider the case of shellular rotation with Ω being a function $\Omega(r)$ of the radius only (Zahn 1992), because in a differentially rotating star the horizontal turbulence is strong enough to ensure a constancy of Ω in latitude. For differentially rotating stars, the structure equations need to be properly written (Meynet & Maeder 1997), which is often not the case in current literature. Structural effects due to the centrifugal force are in general small in the interior, while the distortion of stellar surface may be large enough to produce significant shifts in the HR diagram (Maeder & Peytremann 1970).

Internal transports of chemical elements and angular momentum: For these two transports, we consider the effects of shear mixing, of meridional circulation and their interactions with horizontal turbulence. The equation of evolution of chemical abundances due to the transport and nuclear processes is at each level in lagrangian coordinates (Zahn 1992),

$$\left(\frac{dX_i}{dt}\right)_{M_r} = \left(\frac{\partial}{\partial M_r}\right)_t \left[(4\pi r^2 \rho)^2 (D_{\text{shear}} + D_{\text{eff}}) \left(\frac{\partial X_i}{\partial M_r}\right)_t \right] + \left(\frac{dX_i}{dt}\right)_{\text{nucl}}. \quad (1)$$

The equations of transport of angular momentum in the vertical direction is

$$\rho \frac{d}{dt} (r^2 \Omega)_{M_r} = \frac{1}{5r^2} \frac{\partial}{\partial r} (\rho r^4 \Omega U(r)) + \frac{1}{r^2} \frac{\partial}{\partial r} \left(\rho D_{\text{shear}} r^4 \frac{\partial \Omega}{\partial r} \right). \quad (2)$$

$\Omega(r)$ is the mean angular velocity at level r . $U(r)$ is the radial term of the vertical component of the velocity of the meridional circulation. D_{shear} is the coefficient of shear diffusion. From the two terms in the second member in this last equation, we see that *advection and diffusion are not the same*. Contrarily to what is often made in recent literature, the transport of angular momentum by circulation cannot be treated as a diffusion, (by doing so one may even have the wrong sign for the transport of angular momentum!). For the changes of the chemical elements due to transport, we see that the diffusion coefficient is the sum of D_{shear} and $D_{\text{eff}} = \frac{rU(r)^2}{30D_h}$. D_{eff} expresses the resulting effect of meridional circulation and of a large horizontal turbulence (Chaboyer & Zahn 1992). This expression of D_{eff} tells us that the vertical advection of chemical elements is inhibited by the strong horizontal turbulence characterized by D_h . The usual estimate of the coefficient D_h of horizontal turbulence was $D_h = \frac{1}{c_h} r |2V(r) - \alpha U(r)|$ (Zahn 1992). More recent estimates give higher values for this coefficient (Maeder 2003), confirmed by further studies (Mathis et al. 2004). The diffusion coefficient D_{shear} by shear mixing essentially behaves like

$$D_{\text{shear}} = \frac{(K + D_h)}{\left[\frac{\varphi}{\delta} \nabla_\mu \left(1 + \frac{K}{D_h}\right) + (\nabla_{\text{ad}} - \nabla_{\text{rad}}) \right]} \frac{H_p}{g\delta} \left[\alpha \left(p\Omega \frac{d \ln \Omega}{d \ln r} \right)^2 - 4(\nabla' - \nabla) \right] \quad (3)$$

with $p=0.884$. D_{shear} is also modified by the horizontal turbulence D_h , in the sense that a larger D_h leads to a decrease of the mixing. The radial component $U(r)$ of the meridional circulation is (Maeder & Zahn 1998),

$$U(r) = \frac{P}{\bar{\rho} g C_P \bar{T} (\nabla_{\text{ad}} - \nabla + (\varphi/\delta) \nabla_\mu)} \times \frac{L}{M_\star} [E_\Omega + E_\mu] + \frac{C_P}{\delta} \frac{\partial \Theta}{\partial t}, \quad (4)$$

where $M_\star = M \left(1 - \frac{\Omega^2}{2\pi G \rho_m}\right)$ is the reduced mass, with the notations given in the quoted paper. The driving term in the square brackets in the second member is E_Ω . It behaves mainly like $E_\Omega \simeq \frac{8}{3} \left[1 - \frac{\Omega^2}{2\pi G \bar{\rho}}\right] \left(\frac{\Omega^2 r^3}{GM}\right)$. The term $\bar{\rho}$ means the average on the considered equipotential. The term with the minus sign in the

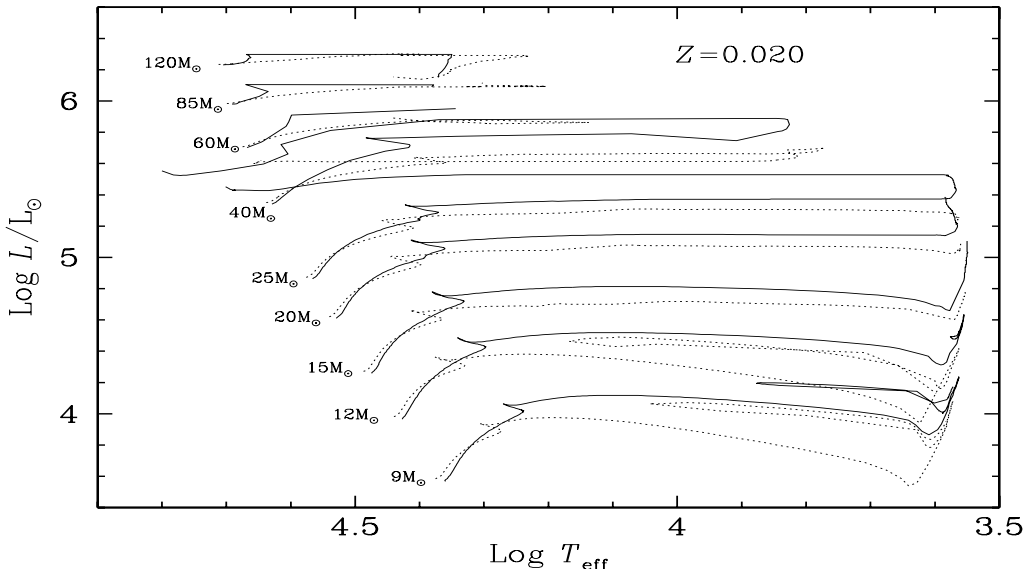


Figure 1. HR diagram of massive stars with $Z=0.02$, for rotating stars with $v_{\text{ini}} = 300$ km/s (continuous lines) and for non-rotating stars (dotted lines).

square bracket is the Gratton–Öpik term, which becomes important in the outer layers when the local density is small. This term produces negative values of $U(r)$, meaning that the circulation is going down along the polar axis and up in the equatorial plane. This makes an outward transport of angular momentum, while a positive $U(r)$ gives an inward transport. At lower Z , the Gratton–Öpik term is negligible, which contributes to make larger Ω -gradients in lower Z stars.

Mass loss in rotating stars: Rotation certainly influences the mass loss rates by stellar winds (Heger & Langer 1998). For a rotating star, one must consider the flux $F(\vartheta)$ at a given colatitude ϑ as given by von Zeipel’s theorem. Thus, in a rotating star, the Eddington factor becomes a local quantity $\Gamma_{\Omega}(\vartheta)$. We define it as the ratio of the local flux $F(\vartheta)$ given by the von Zeipel theorem to the maximum possible local flux, which is $F_{\text{lim}}(\vartheta) = -\frac{c}{\kappa(\vartheta)}g_{\text{eff}}(\vartheta)$. Thus, one has (Maeder & Meynet 2000)

$$\Gamma_{\Omega}(\vartheta) = \frac{F(\vartheta)}{F_{\text{lim}}(\vartheta)} = \frac{\kappa(\vartheta) L(P)[1 + \zeta(\vartheta)]}{4\pi cGM \left(1 - \frac{\Omega^2}{2\pi G\rho_m}\right)}, \quad (5)$$

where the opacity $\kappa(\vartheta)$ depends on the colatitude ϑ , since T_{eff} also depends on ϑ . This shows that the maximum luminosity of a rotating star is reduced by rotation. It is to be stressed that if the limit $\Gamma_{\Omega}(\vartheta) = 1$ happens to be met in general at the equator, it is not because g_{eff} is the lowest there, but because the opacity is the highest!

Often, the critical velocity in a rotating star is written as $v_{\text{crit}}^2 = \frac{GM}{R}(1 - \Gamma)$. This expression is incorrect, since it would apply only to uniformly bright stars. The critical velocity of a rotating star is given by the zero of the equation expressing the total gravity $g_{\text{tot}} = g_{\text{eff}} + g_{\text{rad}} = g_{\text{grav}} + g_{\text{rot}} + g_{\text{rad}}$. This equation has two roots (Maeder & Meynet 2000). The first that is met determines the

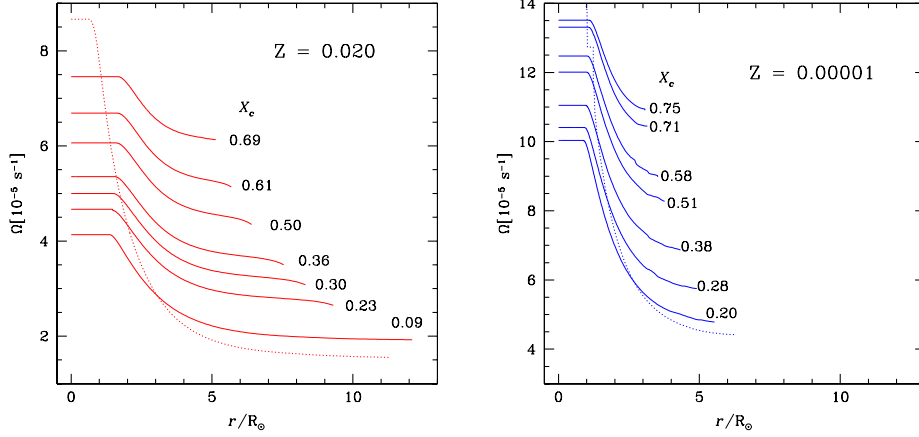


Figure 2. Left: Evolution during the MS phase of the angular velocity Ω in the interior of a $20 M_{\odot}$ star at $Z=0.02$ (Meynet & Maeder 2000). Right: the same for a $20 M_{\odot}$ star at $Z = 10^{-5}$. The values of the central H-content X_c are indicated (Meynet & Maeder 2002).

critical velocity. The first root is as usual $v_{\text{crit},1} = \left(\frac{2}{3} \frac{GM}{R_{\text{pb}}}\right)^{\frac{1}{2}}$, where R_{pb} is the polar radius at break-up. The second root $v_{\text{crit},2}$ applies to Eddington factors bigger than 0.639. It is equal to 0.85, 0.69, 0.48, 0.35, 0.22, 0 times $v_{\text{crit},1}$ for $\Gamma = 0.70, 0.80, 0.90, 0.95, 0.98$ and 1.00 respectively.

The theory of radiative winds applied to a rotating star leads to an expression of the mass flux as a function of colatitude. We may distinguish two effects. a) The “ g_{eff} -effect”: the higher effective gravity makes a higher T_{eff} at the pole and favours polar ejection. For a star hot enough to have electron scattering opacity as the dominant opacity source from pole to equator, the iso-mass loss curve has a peanut-like shape. b) The “opacity-effect”: if the T_{eff} of the star is lower than about 25 000 K, a bistability limit i.e. a steep increase of the opacity (Lamers et al. 1995) may occur somewhere between the pole and the equator, due to the decrease of T_{eff} from pole to equator. This “opacity-effect” produces an equatorial enhancement of the mass loss. The anisotropies of mass loss influence the loss of angular momentum, in particular polar mass loss removes mass but relatively little angular momentum. This may strongly influence the further evolution. We may estimate the mass loss rates of a rotating star compared to that of a non-rotating star at the same location in the HR diagram. The result is (Maeder & Meynet 2000)

$$\frac{\dot{M}(\Omega)}{\dot{M}(0)} \simeq \frac{(1 - \Gamma)^{\frac{1}{\alpha}-1}}{\left[1 - \frac{4}{9} \left(\frac{v}{v_{\text{crit},1}}\right)^2 - \Gamma\right]^{\frac{1}{\alpha}-1}}, \quad (6)$$

where Γ is the electron scattering opacity for a non-rotating star with the same mass and luminosity, α is a force multiplier (Lamers et al. 1995). For B-stars far from the Eddington Limit, $\frac{\dot{M}(\Omega)}{\dot{M}(0)} \simeq 1.5$ For stars close to $\Gamma = 1$ the increase of the mass loss rates may reach orders of magnitude.

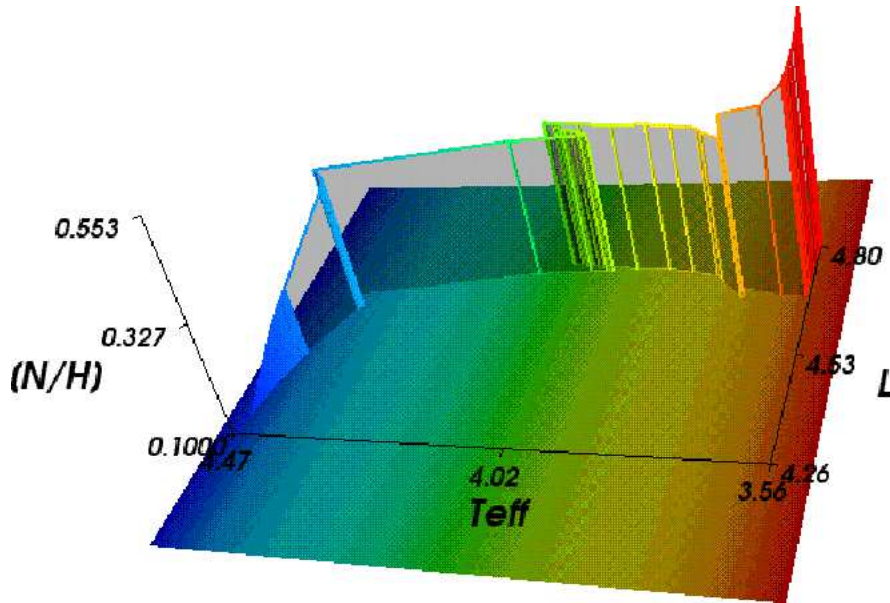


Figure 3. 3-D diagram showing the HR diagram horizontally and N/H on the vertical axis. The values of N/H in number are to be multiplied by 10, they are normalised to the value on the ZAMS. Case of a $15 M_{\odot}$ model with $v_{\text{ini}} = 300$ km/s.

On the whole, there are 3 cases of stellar break-up: 1.- The Γ -Limit, when radiation effects largely dominate; 2.- The Ω -Limit, when rotation effects are essentially determining break-up; 3.- The $\Omega\Gamma$ -Limit, when both rotation and radiation are important for the critical velocity.

3. General results

Grids of models have been made (Meynet & Maeder 2004) at $Z = 0.020$, 0.004 and 10^{-5} . Fig. 1 illustrates the HR diagram for non-rotating and rotating stars at solar metallicity. The rotating models have an initial velocity v_{ini} of 300 km/s, which gives an average velocity of 220 km/s during the MS phase, corresponding to observations. We notice the following points:

- Rotation increases the MS lifetime with respect to non-rotating models (up to about 40 %).
- The values assigned from isochrones with an average rotation velocity typically lead to ages 25% larger than without rotation.
- Rotation strongly affects the lifetimes as blue and red supergiants (RSG). In particular in the SMC, the high observed number of RSG can only be accounted for by rotating models (Meynet & Maeder 2001).

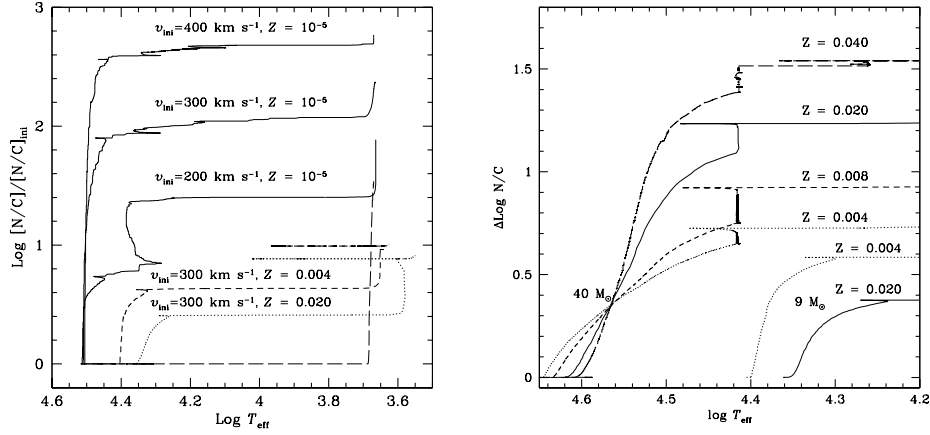


Figure 4. Left: Evolution of the ratio N/C (in number) of nitrogen to carbon for $9 M_{\odot}$ models of different Z and velocities. The ratio are normalized to their initial values. The long-dashed line at the bottom corresponds to a non-rotating model of $9 M_{\odot}$ at $Z = 10^{-5}$. Right: the same at the surface of 9 and $40 M_{\odot}$ models of different Z .

- Steeper gradients of internal rotation Ω are built at lower Z . Fig. 2 shows the evolution during the MS phase of Ω in models at $Z = 0.02$ (left) and at $Z = 10^{-5}$ (right). The steeper Ω -gradient at lower Z favours mixing. There are 2 reasons for the steeper Ω -gradients. One is the higher compactness of the star at lower Z . The second one is more subtle. At lower Z , the density of the outer layers is higher, thus the Gratton-Öpik term is less important. This produces less outward transport of angular momentum and contributes to steepen the Ω -gradient.
- At lower Z , rotating stars more easily reach break-up velocities and may stay at break-up for a substantial fraction of the MS phase.
- There are various filiation sequences for massive stars, as shown below.

$M > 90 M_{\odot}$: O - Of - WNL - (WNE) - WCL - WCE - SN (Hypernova low Z ?)

$60 - 90 M_{\odot}$: O - Of/WNL \Leftrightarrow LBV - WNL(H poor)- WCL-E - SN(SNIIn?)

$40 - 60 M_{\odot}$: O - BSG - LBV \Leftrightarrow WNL -(WNE) - WCL-E - SN(SNIb)
- WCL-E - WO SN (SNIc)

$30 - 40 M_{\odot}$: O - BSG - RSG - WNE - WCE - SN(SNIb)

OH/IR \Leftrightarrow LBV ?

$25 - 30 M_{\odot}$: O -(BSG)- RSG - BSG (blue loop) - RSG - SN(SNIb, SNIIL)

$10 - 25 M_{\odot}$: O - RSG - (Cepheid loop, $M < 15 M_{\odot}$) RSG - SN (SNIIL, SNIIp)

The sign \Leftrightarrow means back and forth motions between the two stages. The limits between the various scenarios depend on metallicity Z and rotation. The various types of supernovae are tentatively indicated.

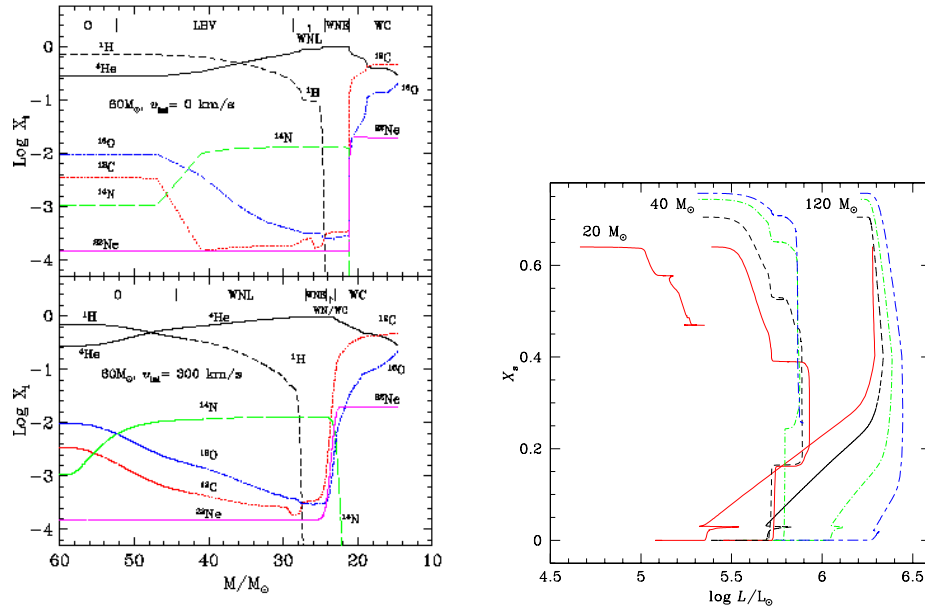


Figure 5. Left: Evolution as a function of the actual mass of the abundances (in mass fraction) at the surface of a non-rotating (upper panel) and a rotating (lower panel) $60 M_{\odot}$ stellar model. Right: Evolutionary tracks in the X_s versus $\log L/L_{\odot}$ plane, where X_s is the hydrogen mass fraction at the surface. The initial masses are indicated. Long-short dashed curves show the evolution of $Z = 0.004$ models, dashed-dotted curves, short-dashed curves and continuous lines show the evolutions for $Z = 0.008$, 0.020 and 0.040 respectively.

4. Evolution of surface abundances in massive stars

4.1. N/C enrichments during the MS phase at various metallicities

As a result of the rotational mixing, products of the CNO processing are reaching the stellar surface during MS evolution and produce N/C enhancements, as observed (Gies & Lambert 1992; Herrero et al. 1992; Lyubimkov 1996) since long in OB-stars. Fig. 3 illustrates in a 3-D plot the growth of N/H on the track of a $15 M_{\odot}$ rotating with an initial rotation $v_{\text{ini}} = 300$ km/s. This velocity corresponds to the average observed velocity during the MS phase of OB stars of about 220 km/s. We see that the N -enrichment progressively occurs during the MS phase, then it keeps about constant during the crossing of the HR and rises up again due to the convective dredge-up in red supergiants.

Fig. 4 left shows the evolution of the N/C ratios in models of rotating stars with $9 M_{\odot}$ for initial $Z = 0.02$, 0.004 and 10^{-5} . At zero rotation, there is no enrichment during the MS phase (except at $Z=0.02$ for $M \geq 60 M_{\odot}$ due to very high mass loss). At $9 M_{\odot}$ for solar Z and an initial rotation of 300 km s^{-1} , the N/C ratio increases by about 0.4 dex during the MS phase. The *relative* values of the N/C ratios increase with decreasing Z , in particular N/C increase by two orders of a magnitude for $Z = 10^{-5}$. This results from the steeper Ω -gradients and greater compactness. Of course, large N/C enhancements are

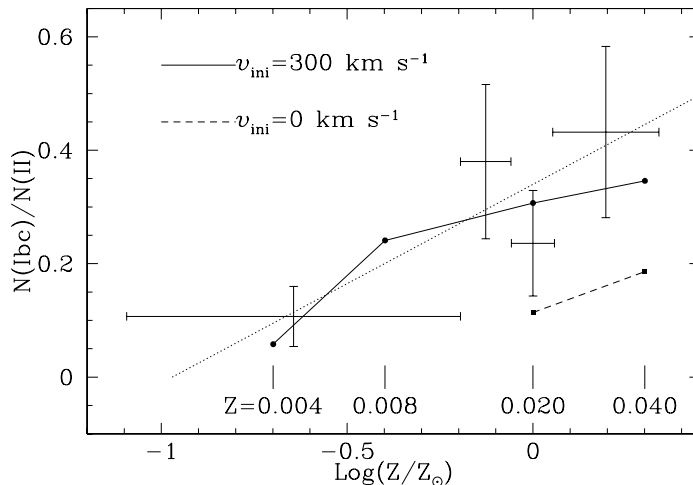


Figure 6. Variations of the number ratios of SN types Ib and Ic with respect to SNIa. The crosses with error bars correspond to observational data (Prantzos & Boissier 2003). The dotted line is a fit proposed by these authors. The continuous and dashed lines show the predictions of rotating and non-rotating models.

accompanied by small enrichments in helium, typically of a few hundredths. The larger N/C enrichments at lower Z have been nicely confirmed by abundances determinations in the SMC (Venn & Przybilla 2004). They found relative N/H enrichments for A-type supergiants in the SMC reaching an order of magnitude or more, while in the Milky Way the enrichments are only by a factor 2 to 3.

During the He-burning phase, the rotation velocities become all the same whatever the initial rotational velocities. Thus, in the He-burning phase we may have very different surface chemical compositions for actually similar rotation velocities.

Fig. 4 right compares the relative N/C enrichments for initial 40 and 9 M_{\odot} stars. For high mass stars ($\geq 30 M_{\odot}$), the higher Z models have the larger enrichments, i.e. a situation opposite to that described above; the reason is that mass loss effects dominate over mixing. Higher Z stars have a higher mass loss, which peels off the stars and make the products of CNO process visible at the stellar surface.

4.2. The abundances in Wolf-Rayet stars

For WR stars, the first major constraint is to explain their relative number ratios to O-type stars, which strongly decrease for lower Z . Rotation makes massive stars to enter earlier in the WR phase and this also increases the lifetimes as WR stars. When account is given to both rotation and to the dependence of the mass loss rates to metallicity Z , the comparisons with observations are greatly improved (Meynet & Maeder 2004).

Fig. 5 left shows the evolution of surface abundances for a 60 M_{\odot} star with and without rotation. Rotation makes smoother changes of abundances, due to internal mixing. For WN stars, the transition phase, when they still have H

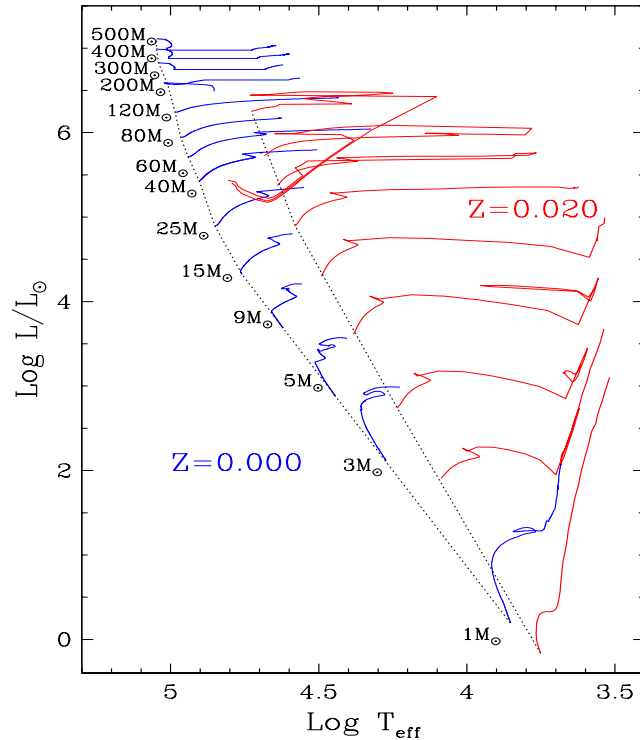


Figure 7. Evolutionary tracks for models at solar and $Z = 0$ (Feijoo 1999).

present, becomes longer due to rotation and this increases the late WN phase (WNL), where H is usually present. The CNO abundances at the end of the WNL phase are the same for rotating and non-rotating models, because they are model independent and determined just by CNO nuclear equilibrium. The same is true for the early WN (WNE), which in general have no or little H present. Indeed, CNO abundances in WN stars provide a unique test of the physics of the CNO cycle.

For the WC phase, the milder composition gradients, when revealed at the surface, make smoother transitions with lower C/He ratios, in good agreement with observations (Crowther et al. 1995). The abundances in WC stars are not equilibrium values, but are products of the partial He-burning, thus they are model dependent and offer a most interesting test on the stellar models. Thus, the abundances in WN and WC stars tell us different stories.

Fig. 5 right shows the evolution of the H-surface content X_s vs. luminosity. This is a very constraining diagram especially for the transition stages from O, Of, LBV to WN stages. It is useful for establishing the proper filiations between such stars. It clearly supports the view that there may be back and forth evolution between LBV and WNL stars, and that in general WN stars succeeds the LBV stage. We also see that descendants from high masses at higher Z significantly decrease in luminosity during their evolution.

The rare WO stars, characterized by a high O/C ratio represent a more advanced stage of nuclear processing. Curiously enough, such stars which may

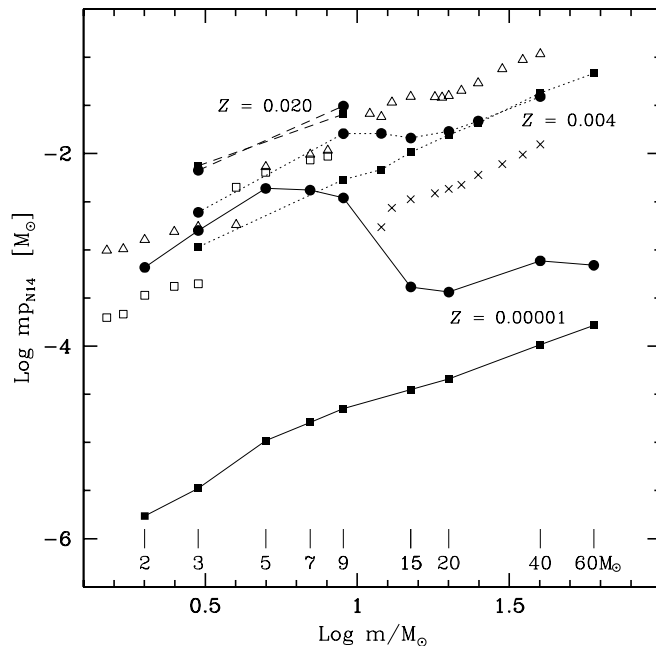


Figure 8. Variation as a function of the initial mass of the stellar yields in ^{14}N for different metallicities and rotational velocities. The continuous lines refer to the models at $Z = 10^{-5}$, the dotted lines show the yields from models at $Z = 0.004$ (Meynet & Maeder 2001), the dashed lines present the yields for solar Z models. The filled squares and circles indicate the cases without and with rotation respectively ($v_{\text{ini}} = 300 \text{ km s}^{-1}$). The crosses are models at $Z = 0.1 Z_{\odot}$ (Woosley & Weaver 1995), the empty squares at $Z = 0.004$ (van den Hoek & Groenewegen 1997) and the empty triangles are for solar Z models (van den Hoek & Groenewegen 1997) up to $8 M_{\odot}$ with complements (Woosley & Weaver 1995).

be the progenitors of supernovae SNIb/c are found only at lower Z . The physical reasons of that have been explained (Smith & Maeder 1991): lower Z stars become WC stars (if they do it) only very late in evolution, i.e. with a high O/C ratio. At the opposite, at higher Z the WC stars may occur at an early stage of He-processing, i.e. with a low O/C ratio. Fig. 6 compares the observed and predicted variations of the number ratio of SNIb or c and SNI and shows an interesting agreement. This is noticeable because of the possible connection WO stars - SNIb/c - GRBs (γ Ray Bursts). In this context, we consider WO stars as good candidate for GRB progenitors.

5. Abundances and yields in very low Z and $Z = 0$ stars

Evolutionary models at $Z = 0$ behave very differently from models at solar composition, as shown by Fig. 7, in particular the evolutionary scenarios and final stages are different (Heger & Woosley 2002). Let us concentrate on the chemical abundances. For metallicities lower than that of the SMC, the internal mixing in intermediate and massive stars is sufficient to bring new C from the

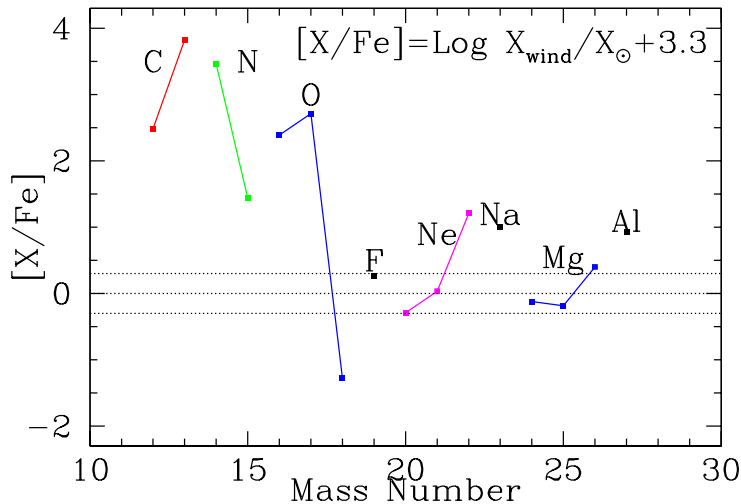


Figure 9. Chemical composition of the matter ejected through stellar winds by a $60 M_{\odot}$ at $Z = 0.00001$ with an initial velocity equal to $2/3$ of the break-up velocity. Note that $\log(Z_{\odot}/Z) = 3.3$ in this diagram. The horizontal dotted lines show the solar ratios (middle) and a factor two enhancement/depletion.

He-burning core to the H-shell where it is then turned to N. This nitrogen is called “primary” as it does not result from CNO elements initially present. Fig. 8 shows the yields in N as a function of the initial mass for $Z = 0.02$, 0.004 and 10^{-5} . At $Z = 0.02$ and $Z = 0.004$ the level of N production is just that resulting from the initial CNO elements, even if at $Z = 0.004$ the N-enrichment is somehow larger than at $Z = 0.02$ (cf. Sect. 4.1). However, at $Z = 10^{-5}$ there is an overproduction of N by 1 or 2 orders of magnitude. This primary N is mainly produced in intermediate mass stars, but the contribution of massive stars is also significant.

Remarkably, at very low Z the fast rotating stars of intermediate masses which reach the TP-AGB phase (this occurs for $M \leq 7 M_{\odot}$) get a higher Z during this phase due to their enrichment in CNO elements. As an example, a $7 M_{\odot}$ has $X(\text{CNO}) = 3.1 \cdot 10^{-3}$ which is 430 times the initial CNO content. Thus very low Z stars may get a higher Z value in post MS phase, which may drive large mass loss rates.

Intermediate and massive stars of low Z easily reach break-up velocities during a significant fraction of their MS phase. This results from the growth of the rotation velocity at their surface, due to the very weak mass loss and to the mild internal coupling (due to meridional circulation) with the contracting core, which spins faster and faster during evolution. As a result of these 2 effects (mass losses at break-up and from higher surface Z), massive rotating stars of very low Z also lose a large fraction of their masses. As an example, a star with an initial mass of $60 M_{\odot}$ at $Z = 10^{-5}$ finishes its life as a $30 M_{\odot}$ core and may possibly lead to an hypernova forming a black hole. The composition of the wind ejecta of this $60 M_{\odot}$ model is illustrated in Fig. 9. It shows large overabundances of C, N and O, as well as lower enrichments in Ne, Na and

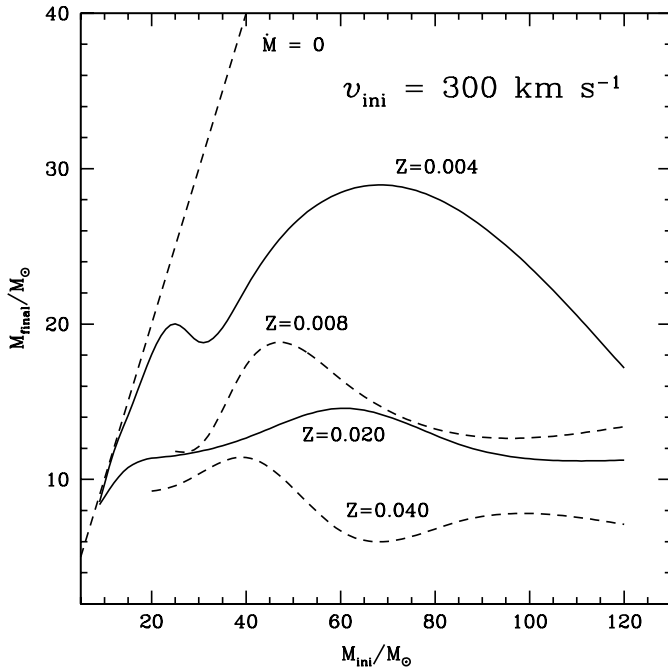


Figure 10. Relation between the final and the initial mass for rotating models at various Z . The final masses of models at very low and zero Z are still uncertain, but they probably significantly differ from the line of those with zero mass loss rate $\dot{M} = 0$.

Al from secondary cycles associated to the CNO cycles. Remarkably, these abundance anomalies well correspond to those observed at the surface of the very metal poor halo stars showing C excess. If there is some other ejecta at the time of the supernova explosion, this material with anomalous abundances will be diluted in the current ejecta with α -rich nuclei.

Thus, we see that if very low Z stars rotate at a significant rate, they may interestingly contribute to account for some abundance anomalies observed in very metal poor halo stars. In this respect, it is interesting to mention that the the ratio of Be-stars to all B stars is 3 to 4 times higher in the SMC than in the solar neighbourhood (Maeder et al. 1999). This suggests that the fraction of fast rotating stars is higher at lower Z .

6. Chemical yields from rotating stars

The relations for various metallicities Z between the final masses at the time of supernovae explosion and the initial stellar masses are still uncertain due to the uncertainties in mass loss rates. The present mass loss estimates lead to the relations illustrated in Fig. 10 for $Z \geq 0.004$. The models are based on the expression of the mass loss rates as a function of metallicity given by $\dot{M}(Z) = \dot{M}(Z_{\odot}) (Z/Z_{\odot})^{\alpha}$ (Kudritzki 2002), a relation which is certainly different in the various evolutionary phases, since the mechanisms of mass loss are not the same.

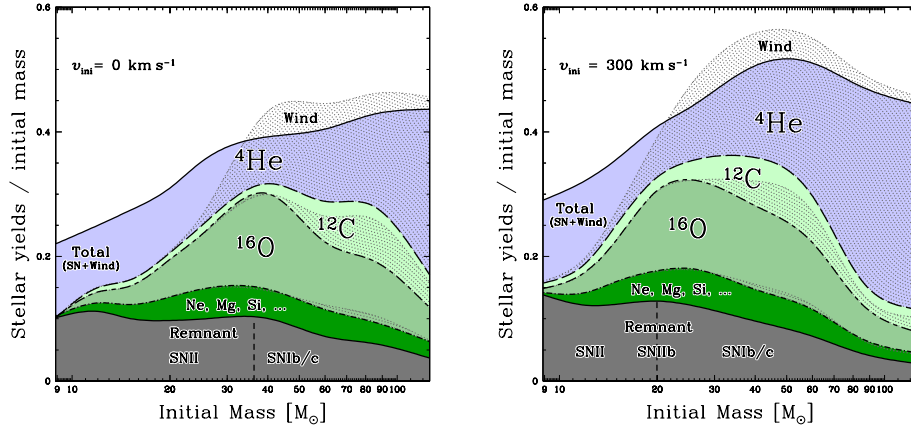


Figure 11. Left: The chemical yields for models without rotation. Right: The chemical yields for models with $v_{\text{ini}} = 300 \text{ km/s}$ (Hirschi et al. 2004).

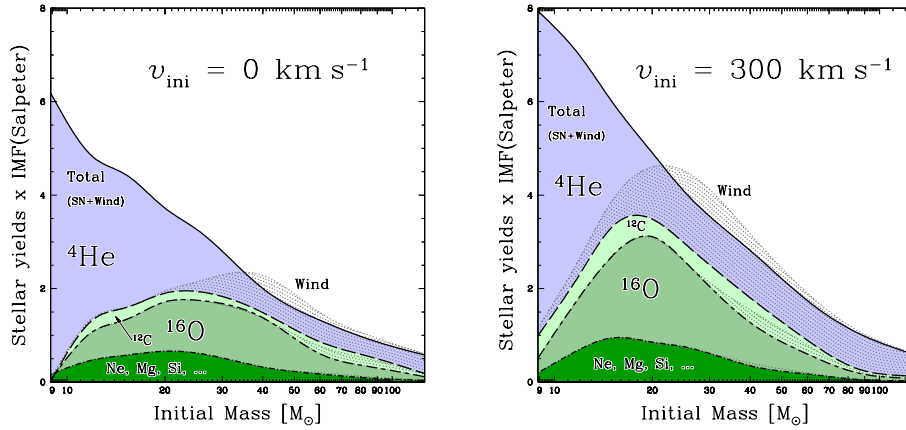


Figure 12. Left: The yields x IMF for models without rotation. Right: The yields x IMF for models with $v_{\text{ini}} = 300 \text{ km/s}$ (Hirschi et al. 2004).

For the very low and zero Z , the uncertainties are still too large, so that we do not know the final masses. However, we emphasized above that, in very low Z stars, surface enrichments due to internal mixing may enhance the mass loss by stellar winds, also the stars may reach break-up and experience significant mass loss. The values of the final masses are critical for determining the types of supernovae and also for nucleosynthesis, because as is evident what is escaping in the winds is not further nucleary processed.

The model evolution of rotating stars has been pursued up to the presupernova stage (Hirschi et al. 2004), since we know that nucleosynthesis is also influenced by rotation (Heger et al. 2000). Fig. 11 show the chemical yields from models without and with rotation. Fig. 12 shows these yields multiplied by the initial mass function (IMF). The main conclusion is that below an initial mass of $30 M_{\odot}$, the cores are larger and thus the production of α -elements is

enhanced. Above $30 M_{\odot}$, mass loss is the dominant effect and more He is ejected before being further processed, while the size of the core is only slightly reduced. When we account for the weighting by the IMF, the production of oxygen and of α -elements is globally enhanced as illustrated by Fig. 12, while the effect on the He-production in massive stars remains limited. It will be interesting to explore the consequences of these new yields for the chemical evolution of the Galaxy.

As a general conclusion, we see that the chemical abundances at all stages are a most constraining test of stellar evolution and in particular of the internal mixing process and of mass loss, which are effects strongly influencing all the outputs of evolution and nucleosynthesis.

References

- Chaboyer, B., Zahn, J.P. 1992, A&A 253, 173
 Crowther, P.A., Smith, L.J., Willis, A.J. 1995, A&A 304, 269
 Feijoo, J.M. 1999, Internal report, Diploma work, Geneva Observatory.
 Gies, D.R., Lambert, D.L. 1992, ApJ 387, 673
 Heger, A., Langer, N. 1998, A&A 334, 210
 Heger, A., Woosley, S.E. 2002, ApJ, 567, 532
 Heger, A., Langer, N., & Woosley, S. E. 2000, ApJ, 528, 368
 van den Hoek L.B., Groenewegen M.A.T. 1997, A&ASS 123, 305
 Herrero, A., Kudritzki, R.P., Vilchez, J.M. et al. 1992, A&A, 261, 209
 Hirschi, R., Meynet, G., Maeder, A. 2004, A&A, in press
 Kudritzki, R.P. 2002, ApJ, 577, 389
 Lamers, H.J.G.L.M., Snow, T.P., Lindholm, D.M. 1995, ApJ 455, 269
 Lyubimkov, L.S. 1996, Ap&SS, 243, 329
 Maeder, A. 2003, A&A 399, 263
 Maeder, A., Grebel, E., Mermilliod, J.C. 1999, A&A 346, 459
 Maeder A., Meynet G. 2000, A&A 361, 159 (paper VI)
 Maeder A., Meynet G. 2001, A&A 373, 555 (paper VII)
 Maeder A., Peytremann, E. A&A, 7, 120
 Maeder A., Zahn, J.P. A&A, 334, 1000
 Mathis, S., Palacios, A., Zahn, J.P. 2004, A&A, in press
 Meynet G., Maeder A. 1997, A&A, 321, 465 (Paper I)
 Meynet, G., Maeder, A. 2000, A&A, 3, 101 (paper V)
 Meynet G., Maeder A. 2002, A&A, 390, 561 (paper VIII)
 Meynet G., Maeder A. 2004, A&A, in press(Paper XI)
 Prantzos, N., Boissier, S. 2003, A&A 406, 259
 Smith, L.F., Maeder A. 1991, A&A, 241, 77
 Venn, K., Przybilla, N. 2003, in *CNO in the Universe*, Eds. C. Charbonnel et al., ASP Conf. Ser. 304, p. 20.
 Woosley S.E., Weaver T.A. 1995, ApJS 101, 181
 Zahn J.P. 1992, A&A 265, 115